Available online at www.sciencedirect.com
SCIENCE DIRECT
Cement & Concrete Composites 28 (2006) 393–401
Cement & Concrete Composites
www.elsevier.com/locate/cemconcomp

Application of impulse-thermography for non-destructive assessment of concrete structures

Ch. Maierhofer [a,*], R. Arndt [a], M. Röllig [a], C. Rieck [b], A. Walther [c], H. Scheel [c], B. Hillemeier [c]

[a] Federal Institute for Materials Research and Testing (BAM), Division VIII.2, Unter den Eichen 87, D-12205 Berlin, Germany
[b] Institute for Material Testing MPA of Berlin-Brandenburg Voltastraße 5, 13355 Berlin, Germany
[c] Technical University of Berlin, Department of Building Materials and Building Material Examination, Gustav-Meyer-Allee 25, Secr. TIB1-B4, 13355 Berlin, Germany

Abstract

Impulse-thermography is an active method for quantitative investigations of the near surface region of various structures. It has recently been applied and optimised to applications in civil engineering. By using either an internal or external heat source, parts of the structure under investigation are heated up and the transient heat flux is observed by recording the temperature change at the surface as a function of time. This method is very well suited for the detection of voids and honeycombing in concrete, up to concrete covers of 10 cm as well as for the location of delaminations in multi-layered systems (e.g. plaster on concrete, CFRP-laminates on concrete, asphalt on concrete). Also safety relevant defects like voids in tendon ducts and cracks in concrete could be recognised.

Keywords: Non-destructive testing; Impulse-thermography; Concrete; CFRP-laminates; Delamination; Tendon duct; Voids; Compaction faults

1. Introduction

During the last 10 years, advanced non-destructive testing (NDT) methods like radar, ultrasonics and impact-echo have become available for concrete and masonry structures and can be used for the assessment of existing structures [1,2]. These technologies are mainly suited for the detection and characterisation of inhomogeneities in concrete and masonry structures at depths (e.g. concrete cover) between 5 and 100 cm. In the near surface region between 0 and 10 cm, there is still a deficiency of information, which can be remedied with impulse-thermography [3,4]. In contrary to the well-known passive investigations of the quality of thermal insulation of building envelopes [5], impulse-thermography is based on the active heating of structures to be investigated. By using either an internal or external heat source, parts of the structure under investigation are heated up and the transient heat flux is observed by recording the temperature change at the surface as a function of time. The differences between temperature transient curves at surface positions above non-defect regions and inhomogeneities are expected to include information about the defect parameters like depth, lateral size and the type of material. Defects like voids in concrete or masonry or delaminations at interfaces of composites, which have different density, heat capacity and/or heat conductivity in comparison to the bulk material, can be localised and partly quantified.

The analysis of heating-up and cooling-down processes during and after activation with an internal or external heat source (i.e. radiator) is a well-established technique for the characterisation of non-metallic materials [6,7]. Up to now, there are only a few examples where active thermography has been applied successfully in civil engineering [8]. The method is very useful for the determination of the built-in position of anchoring elements at curtain facades as well [9]. Further developments and applications in civil engineering are using the sun as a natural heat

* Corresponding author. Tel.: +49 30 8104 1441; fax: +49 30 8104 1447.
E-mail address: christiane.maierhofer@bam.de (Ch. Maierhofer).

0958-9465/$ - see front matter © 2006 Elsevier Ltd. All rights reserved.
doi:10.1016/j.cemconcomp.2006.02.011

source. Examples are inspections of bridge decks [10] and of paving in general [11]. For locating delaminations at bridge decks, an ASTM standard, published in 1988 with the title *Standard Test Method for Detecting Delaminations in Bridge Decks Using Infrared Thermography* [12], exists. Laboratory investigation of plaster detachments have been performed by [13].

Recently, the Technical University of Berlin and BAM have performed systematic investigations for several possible applications in civil engineering in a project funded by the DFG (Deutsche Forschungsgemeinschaft, *German Research Council*). Testing problems which were analysed within the project so far were the localisation of voids and honeycombing in concrete elements including the influence of moisture, of varying reinforcement and concrete material properties, of delaminations of plaster on concrete and masonry, of adhesive bond defects between carbon fibre reinforced plastic (CFRP) laminates and concrete, of voids inside tendon ducts and of dry and moist cracks. Despite a large amount of laboratory tests under varying conditions, several on-site measurement campaigns have been performed successfully.

2. Experimental

2.1. Impulse-thermography

For actively heating the surface of the structure to be investigated, different kinds of heating units including radiant and fan heaters, flash and halogen lamps can be applied.

One experimental set-up for the performance of impulse-thermography measurements in laboratory as well as on-site is shown in Fig. 1(left). It consists of a thermal radiator, an infrared camera and a computer system that enables digital data recording in real time. The thermal heating unit contains of three infrared radiators having a power of 2400 W each. The heating procedure is usually done dynamically by moving the radiators under computer control to obtain the best possible homogeneous heating. Therefore, radiators are mounted in a linear array and are moved vertical to this array and parallel to the surface at a distance of about 15 cm.

For the location of injection faults inside tendon ducts, the pre-stressing steel is heated up by a welding apparatus with electric currents between 15 A and 50 A, using the electric resistance of the pre-stressing wire as shown in Fig. 1(right). Inside the ducts, maximum temperatures of 25 °C were recorded with thermocouples.

2.2. Data analysis

2.2.1. Thermal contrast

For qualitative data analysis, thermograms of experimental data recorded at different time intervals after heating were selected. The grey values of the images were scaled to minimum and maximum temperature in each image. Shallow defects have maximum thermal contrast after short cooling-down time while deeper defects appear later.

For quantitative analysis, transient curves (surface temperature as a function of time for each pixel (i,j)) from areas above defects and above homogeneous bulk material were compared and difference curves were calculated as shown in Fig. 2. These difference curves usually have a maximum $\Delta T_{\max}$ at a distinct time $t_{\max}$ that depend on the depth and size of the defects, on the heating time and of course on the thermal properties of bulk and defect material. For further data interpretation and for solving the inverse problem, a numerical simulation program was adapted and developed based on finite differences and the differential equation of Fourier [4]. Further simulations have been performed by using a finite element program [14].

2.2.2. Pulse-phase-thermography

Pulse-phase-thermography (PPT) is based on the analysis of the above-mentioned transient curves in frequency domain. Basic research on PPT has been accomplished in

Fig. 1. Left: experimental set-up with infrared camera, computer and infrared radiator for direct heating of the surface. Right: electrical connections at the wires inside the tendon ducts for indirect heating by electric resistance.

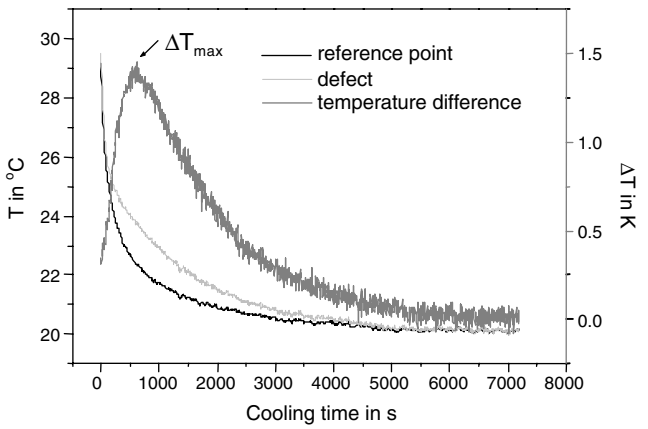

Fig. 2. Temperature as a function of time (transient curves) above a defect (void) inside a concrete test specimen and above a reference area close to the defect during cooling down. Also the temperature difference curve with a maximum thermal contrast of ΔT_{max} is shown.

the group of Maldague, which reports about principles of PPT [15]. In this paper, the method was tested on specimens made from aluminium and different kind of polymers. Each pixel (i,j) of a series of thermal images describing the cooling-down behaviour after heating is analysed by application of the Fourier transformation. One obtains amplitude and phase images for different frequencies.

Amplitude images show the internal structure of a specimen up to a maximum available depth depending on the frequency (low pass filter behaviour). Phase images show the internal structure within a certain depth range depending on the frequency (band pass filter behaviour).

The main advantages of PPT are given by the following properties of the phase images:

- Deeper probing as for amplitude images and thus enhanced detectability.
- Phase images are less influenced by surface infrared and optical characteristics and less sensitive to non-uniform heating than thermal images and amplitude images.
- Enhanced resolution of defect geometry.
- Non-necessity to know a priori the position of non-defect area. This pre knowledge is required for the computation of contrast images and difference curves.

In Fig. 3, the amplitude and phase spectra processed from the transient curves in Fig. 2 are displayed. In our experiment, the heating pulse is represented as a square pulse, which can be described as superposition of different frequencies with varying amplitudes. The available energy is concentrated in the low frequencies. The pulse duration determines the frequency spectrum in that way, that for longer pulses lower frequencies contain more energy and therefore more information. This is exceedingly true for the long pulse durations necessary for the investigation of concrete for up to 1.5 h [16]. The maximum frequency is determined by the acquisition rate, the minimum frequency is limited by the recording time. In practice only the first images at low frequencies are of interest, since most of the energy is concentrated here. Higher frequencies exhibit a higher noise level.

3. Results of laboratory investigations

3.1. Location of voids in concrete

3.1.1. Influence of void size and depth

The detectability of voids in concrete by using active impulse-thermography is influenced by the size and depth of the voids. To investigate this influence, a concrete test specimen was built as demonstrated in Fig. 4, having a size of $1.5 \times 1.5 \times 0.5$ m^3. Before concreting, eight voids, simulated by polystyrene cuboids with sizes of $20 \times 20 \times 10$ cm^3 and $10 \times 10 \times 10$ cm^3, were positioned by polyamide threads in the wooden formwork. Additionally the polystyrene cuboids were fixed with wooden bars to avoid surfacing during concreting. Inside the table in Fig. 4, the intended depths for incorporation as well as data obtained from radar measurements are given. Some of the polystyrene cuboids (defects number 3 and 4) are not oriented parallel to the surface, but have a tilted orientation.

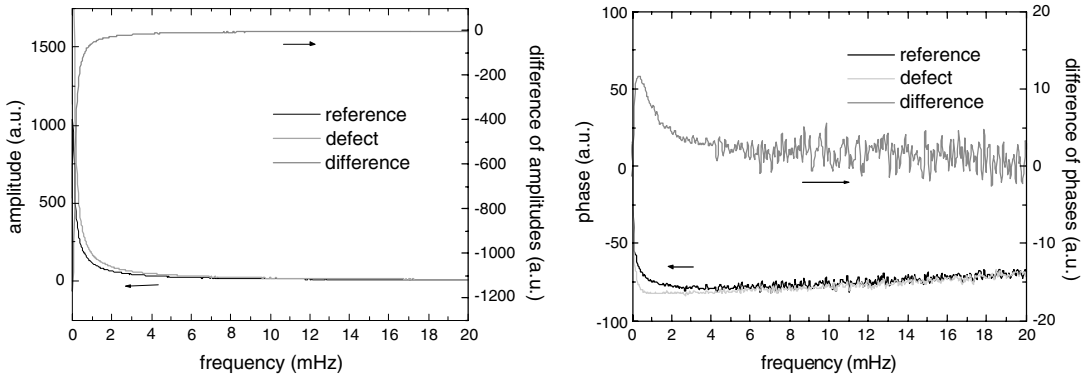

Fig. 3. Amplitude spectra (left) and phase spectra (right) of transient curves above the defect and reference area. Also displayed is the respective difference curve in each diagram.

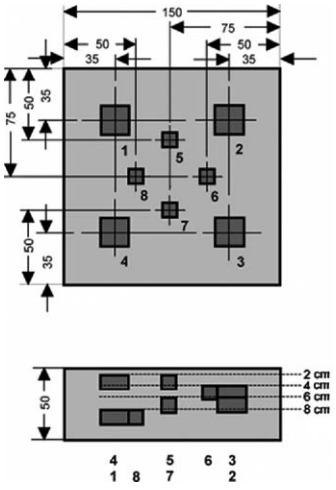

Number of defect	Intended concrete cover	Radar result on concrete cover
1	8 cm	9.2±1.5 cm
2	6 cm	7.6±1.5 cm
3	4 cm	4.0±1.0 cm
4	2 cm	1.0±1.0 cm
5	2 cm	3.0±1.0 cm
6	4 cm	4.3±1.0 cm
7	6 cm	3.5±1.0 cm
8	8 cm	4.3±1.0 cm

Fig. 4. Concrete test specimen including polystyrene cuboids with different sizes at different depths. All data without units are in cm. The drawing is not scaled. The table contains nominal size and depth (concrete cover) of polystyrene cuboids inside the concrete test specimen and concrete cover determined with radar.

For systematic investigation of this concrete test specimen, six measurement cycles were recorded with various heating times from 5 to 60 min. The infrared camera had a distance of 2.8 m and a height of 0.82 m enabling the observation of an area with a size of 1.5×1.5 m^2. All thermal images were recorded at a rate of 2 frames per second.

In Fig. 5(top) selected thermograms of the measurement cycle with 30 min of heating are shown. In each image, the temperature is scaled to the respective minimum and maximum to obtain the best possible contrast. It can be seen that the small voids (No. 5–8), which are covered by 3–4.5 cm by concrete as well as the shallow larger voids (No. 3 and 4) are visible with maximum contrast at the beginning of the thermal sequence (13.3 min after switching off the heating source). With increasing observation time, the deeper large voids (No. 1 and 2) appear, while the contrast of the other voids decreases.

The respective phase images of this thermal sequence are displayed in Fig. 5(bottom). At the lowest frequency of 0.14 mHz, all voids can be clearly seen with a higher

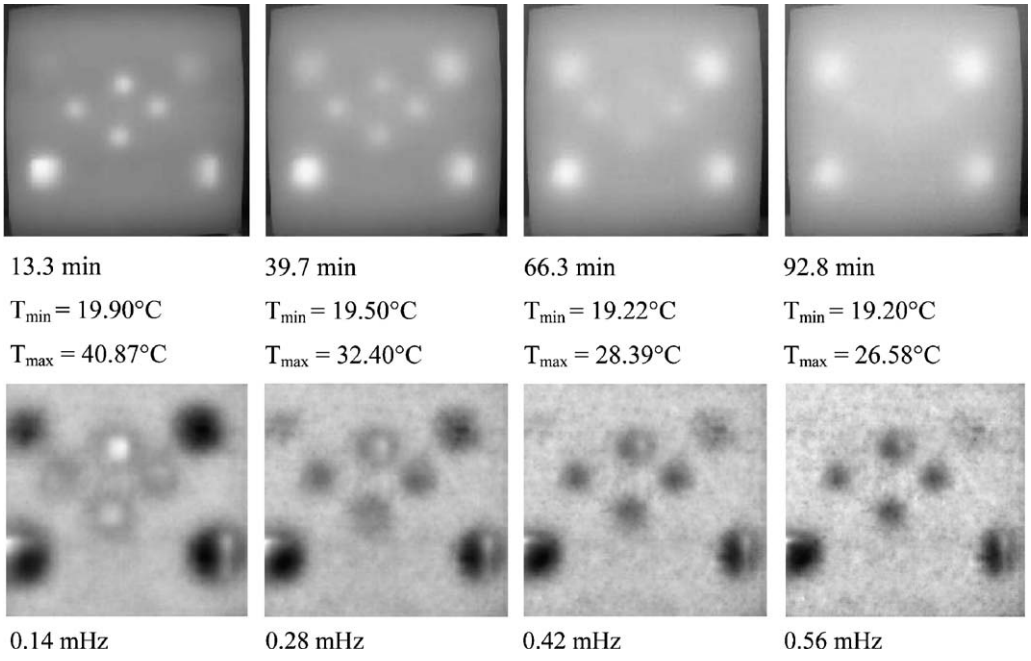

Fig. 5. Comparison of thermograms (top) and phase images (bottom) of voids at different depths simulated by polystyrene cuboids inside a concrete test specimen. The heating time was 30 min, the recording time of the thermograms is related to the switch off time (0 s) of the heating source.

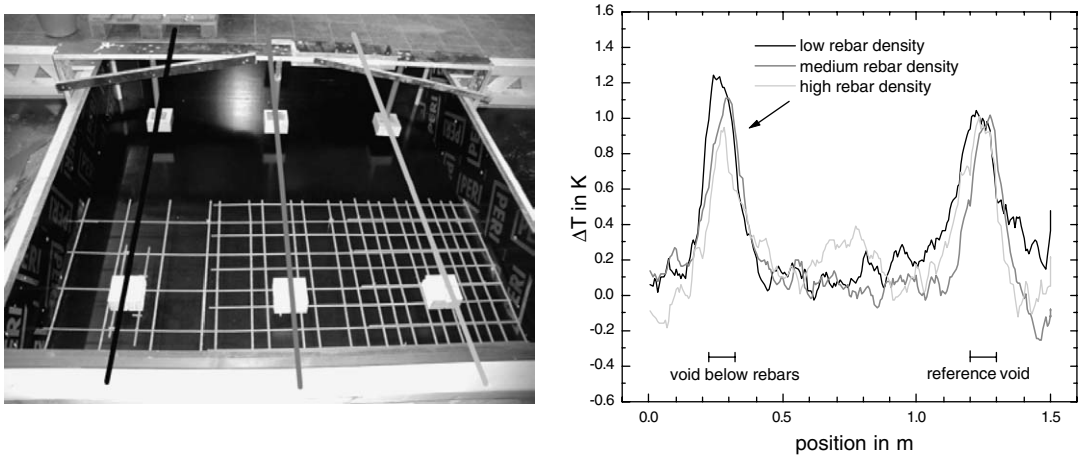

Fig. 6. Left: test specimen with voids and different number of reinforcement mats before concreting. Right: temperature distribution at the surface of the test specimen along the measurement lines depicted in the left image.

signal-to-noise ratio as in the thermograms. For higher frequencies, the deeper voids (No. 1 and 2) disappear and cannot be seen any more at a frequency of 0.56 mHz. The voids with a tilted orientation in respect to the surface (No. 3 and 4) appear half black and half white. It can be deduced that one corner is much deeper than the other. This effect is in accordance with a better geometrical resolution of phase images.

3.1.2. Influence of reinforcement density

For the investigation of the influence of reinforcement density, a test specimen was constructed as displayed in Fig. 6(left). It has three voids with a size of $10 \times 10 \times 5$ cm^3 (simulated by polystyrene) at a depth of 6 cm and located behind three different densities of reinforcement (one, two and three layers of reinforcement mats Q188, 1.88 cm^2 reinforcing steel per m). At the same height and depth, three further reference voids (also simulated by polystyrene and having the same size) without any reinforcement were included.

Data obtained from the observation of the cooling-down behaviour after a heating duration of 30 min are shown in Fig. 6(right). The thermograms showing the maximum temperature contrast above the voids were selected and three horizontal line scans were taken across the areas of different reinforcement density. Each of these scans included a void below the reinforcement and a reference void. Only a small influence of the rebar density could be noticed: with increasing rebar density, the temperature contrast of the underneath voids decreases slightly.

3.1.3. Influence of concrete material properties

It is expected that variations of concrete mixture have an influence on the density, thermal conductivity and heat capacity of the hydrated concrete and thus on the detection of voids. For systematic investigations, three concrete test specimens with a size of $1.0 \times 1.0 \times 0.3$ m^3 with at least one polystyrene cuboid with a size of $10 \times 10 \times 5$ cm^3 at a depth of 6 cm have been constructed with different content of pores in cement matrix and porosity of aggregates as shown in Table 1.

Numerical simulations have been performed for a void with a size of $10 \times 10 \times 5$ cm^3 at a depth of 6 cm embedded in concrete for varying thermal conductivities (Fig. 7(left)) and varying densities (Fig. 7(right)). These curves show that an increase of thermal conductivity should lead to a small variation of ΔT_{max} and to a large decrease of t_{max}. The reduction of the density has a larger influence on ΔT_{max} and a smaller influence on t_{max}. Comparing the theoretical values with the experimental results in Table 1, for specimen No. 2, ΔT_{max} increases clearly while t_{max} slightly decreases (within measurement accuracy) related to the values of specimen No. 1. Therefore, the reduction of density and not the reduction of thermal conductivity has a main influence on the data here. For specimen No. 3, the experimental values of ΔT_{max} as well as t_{max} increase

Table 1
ΔT_{max} and t_{max} of the transient curves above void 2 for the different test specimen after a heating time of 30 min

Concrete type (No.)	Air content in fresh concrete (vol%)	Density (kg/dm^3)	Compressive strength of cubes (N/mm^2)	t_{max} (s)	ΔT_{max} (K)
Normal (1)	0.9 ± 0.2	2.33 ± 0.03	48.5 ± 2.0	900 ± 50	1.72 ± 0.08
Air-entraining agents (2)	3.9 ± 0.2	2.28 ± 0.03	37.6 ± 2.0	880 ± 50	2.57 ± 0.08
Porous aggregates (3)	6.0 ± 0.2	1.85 ± 0.03	27.4 ± 2.0	1290 ± 70	2.18 ± 0.08

Compressive strength and density were determined at 28 days old cubes.

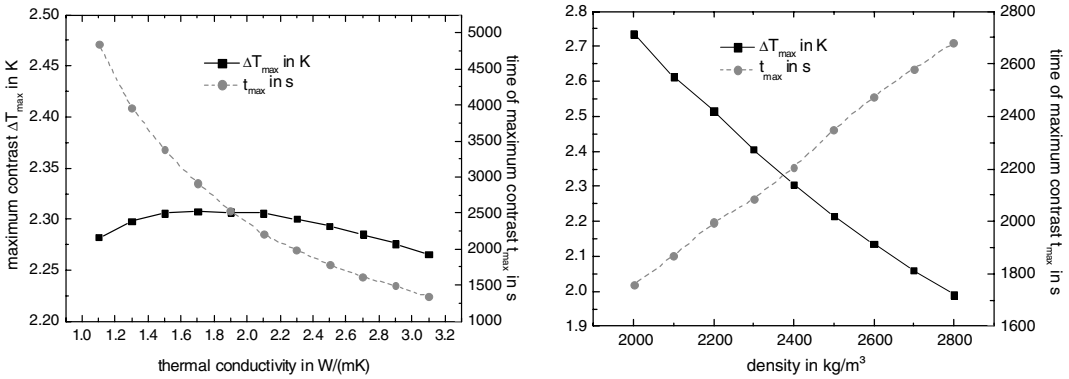

Fig. 7. Simulated maximum temperature differences ΔT_{max} and time t_{max} for a 6 cm deep polystyrene block depending on thermal conductivity (left) and density (right) of bulk concrete (simulated heating duration: 30 min).

clearly. Here, the effects of increased density and increased thermal conductivity superimpose each other.

3.2. Location of delaminations of CFRP-laminates on concrete

For subsequent reinforcement of concrete structures, the application of carbon fibre reinforced plastic (CFRP) laminates was raised during the last years. Here, the bonding between the laminates and the concrete is essential, which can be easily tested with impulse-thermography. For systematic investigation, a homogeneous concrete test specimen ($1.5 \times 1.5 \times 0.5\ m^3$) was constructed. Three months after concreting, nine carbon fibre reinforcing laminate stripes were glued at the surface of one side with varying glue thickness. Areas without glue should simulate delaminations with different sizes as shown in Fig. 8(left).

These delaminations can already be detected after a heating time of 15 s by using the thermal radiator (Fig. 8(right)). Beside the nominal defects, several additional small inhomogeneities can be detected at all stripes that are not related to an inhomogeneous surface but to small unintentional delaminations. Especially at the 5th stripe from the top, two additional delaminations can be detected at the edges of the different glue thicknesses. The analysis of the transient curves shows that the maximum temperature difference is similar for all delaminations. An influence of glue thickness cannot be found.

3.3. Detection of voids inside tendon ducts

In order to protect pre-stressing steel against corrosion, tendon ducts in pre-stressed concrete constructions are grouted with cement paste. Ungrouted areas endanger the durability of pre-stressed concrete constructions. Larger grouting faults are usually located at higher parts of the tendon, where the concrete covering of the ducts is often small (down to 5 cm) as shown in Fig. 9. Therefore, in these cases the corrosion protection is not given any more.

In order to examine the applicability of impulse-thermography for the detection of grouting faults inside ducts, 3.50 m long sample test specimens were constructed consisting of reinforced concrete with two tendon ducts including tendon wires as shown in Fig. 10. Inside the tendon ducts having a diameter of 80 mm, in each case three non-grouted areas with a length of 45 cm each were integrated. The tendon ducts had a concrete cover of 8 cm from one side and of 5 cm from the other side.

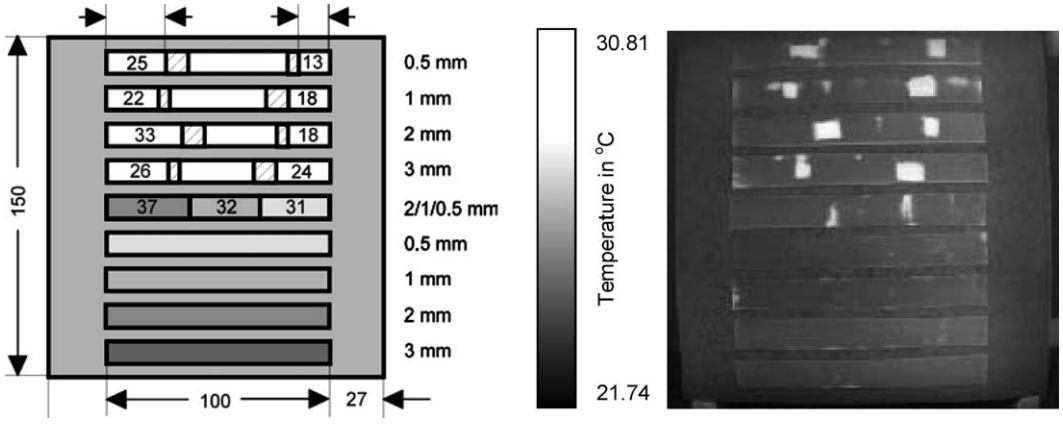

Fig. 8. Left: test specimen with carbon fibre reinforced plastic laminates, which have no contact at the shaded areas (nominal glue thickness is written on the right side). Right: thermogram directly recorded after a heating time of 15 s.

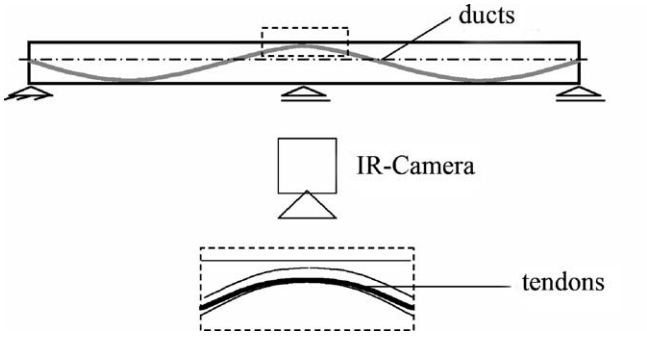

Fig. 9. Grouting faults inside ducts are often located at the highest part of the tendons, where it is possible to detect these with impulse-thermography.

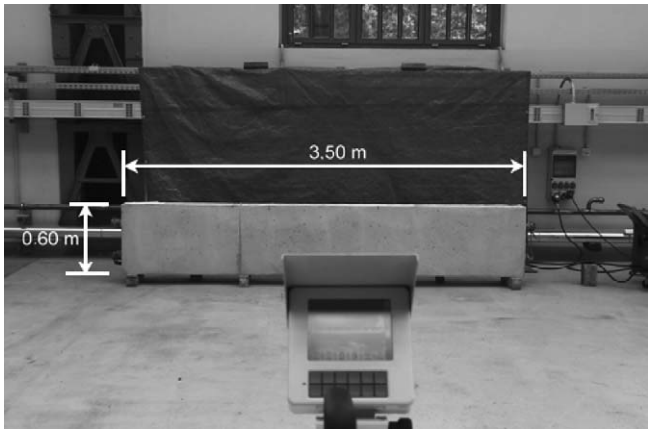

Fig. 10. Experimental setup for internal heating of the tendon wires: the electrodes of the transformer are connected to the pre-stressing strands by copper wire.

Transient temperature distributions for detecting these non-grouted areas were realised in three different ways.

In the first case, the heat during hydration of the cement inside the ducts was used. Few minutes after grouting, the ducts could be detected at the surface with the infrared camera. Likewise the grouting faults could be located.

In the second case, the pre-stressed concrete test specimen was heated up to 15 min from the outside surface by infrared radiators with a total electrical connected load of 5200 W. Only from the side with small concrete covering ($c = 5$ cm) the grouting faults in the ducts could be detected clearly.

In the third case, the heat impulse was generated internally by conductive heating of the wires inside the ducts (Fig. 10). By means of a transformer, a current of 15 A was applied for a duration of 15 min. The thermogram in Fig. 11 was taken up about 40 min after the beginning of heating. Along both tendon ducts, warm and cold areas appear corresponding to the grouted and non-grouted areas, respectively. The electrical contacts appear with the highest temperature due to the transition resistance. The temperature within the ducts was measured with thermocouples and rose up by approx. 5 K.

4. On-site tests

4.1. Location of asphalt delaminations on a concrete bridge

On-site-investigations on a pre-stressed concrete bridge were carried out for the detection of voids or delaminations inside or below the top asphalt layer. The paving above the concrete plate consisted of up to 50 mm concrete for equalisation, 10 mm mastic for sealing and an asphalt layer with a thickness of 50 mm. Thermal images were taken at varying times after sunrise, thus using the sun as heating source.

Fig. 12 shows a thermogram taken at 10:00 a.m. at a measured solar radiation of 800 W/m^2. Clearly distinguishable are areas of higher temperature that might be related to defects or delaminations. The largest of these areas in

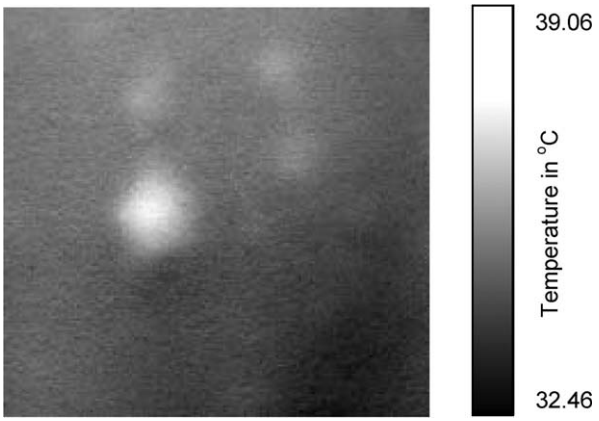

Fig. 12. Thermogram recorded at 10:00 a.m. summer time, 2005-06-23, sunny, in Berlin, of a 1×1 m^2 sized area of an asphalt layer on a concrete bridge. The delaminations are clearly shown as warmer areas.

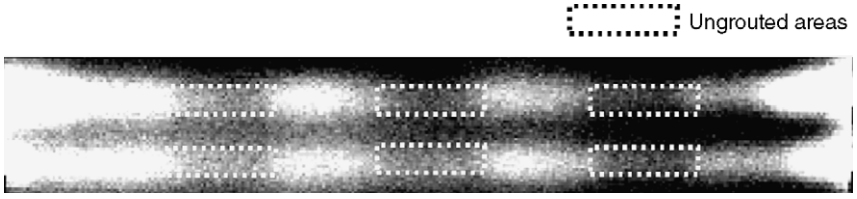

Fig. 11. Temperature distribution, 40 min after switching on of the heating source (white: temperature > 16.0 °C, black: temperature < 14.5 °C). The six ungrouted areas are colder than the grouted areas of the two horizontal tendons.

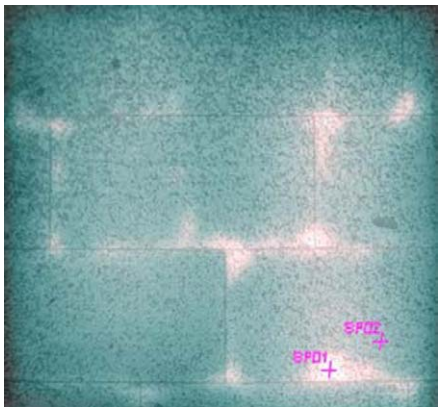

Fig. 13. Super positioning of an equalised digital photo and the related equalised thermogram of several granite tiles (total area 1×1 m^2) recorded after a heating time of 3 min. The voids could be clearly detected as warmer (white) areas.

the middle of Fig. 12 has a temperature difference of 3.5 K to its surrounding.

4.2. Voids below a stone floor

For the detection of voids below a stone pavement consisting of granite tiles with a thickness of 1.5 cm, which were laid on mortar on a concrete floor, a whole area of 40 m^2 was investigated. Single areas of about 1 m^2 were heated up with an infrared radiator for about 3 min. The cooling-down behaviour was recorded with the infrared camera. The voids could be easily detected with a temperature difference of about 2.5 K as shown in Fig. 13. Here, the super positioning of the photogrammetric equalised digital photo as well as of the equalised thermogram recorded 1.33 min after switching of the heating source is displayed.

5. Summary and outlook

The demonstrated results recorded at test specimens and on-site clearly show that impulse-thermography is very well suited for the visualisation of inhomogeneities and defects close to the surface (up to a depth of 10 cm) of building structures. By inducing a non-stationary temperature distribution, the analysis of temporal temperature data in time and frequency domain (e.g. pulse-phase-thermography) enables the detection of inhomogeneities in concrete structures, masonry and multi-layered systems with high reliability.

For proofing defects at larger depths, like ungrouted areas in tendon ducts, long measurement times up to 1.5 h are required, but for defects up to 2 cm, a few minutes or less heating time is needed.

At time, impulse-thermography is not applied regularly for on-site testing, most investigations were carried out in the laboratory. However, the measurement equipment including radiator, infrared camera and computer can be applied at the building site without major modifications. The main requirement is the accessibility of the surface of the structure under investigation. A direct contact to the surface is not required. A limit of the maximum surface temperature should be set for avoiding any damages due to heating.

The data gained about the inhomogeneities are only semi-quantitative, i.e. only the lateral position and dimension could be determined from the images. More information about the material properties and the depth of the inhomogeneities can only be obtained by comparing the experimental data to calibration curves or numerical simulations. Furthermore, for quantitative analysis it has to be considered that the structure under investigation might be out of thermal equilibrium at the beginning of the experiments, e.g. due to heating of the internal space while investigating an exterior wall or due to the influence of solar radiation.

Also the sun could be used as an active heating source as outlined in the example of the investigation of the highway bridge in this paper. Here, asphalt delaminations could be detected with relatively high thermal contrast.

Impulse-thermography could be applied for quality assurance during construction and after reconstruction as well as for regular and exceptional building assessment.

Acknowledgements

We gratefully acknowledge Dipl.-Ing. Uwe Meinhold from BAM VII.1 for supporting the construction of the test specimen and Dr. Matthias Hemmleb from BAM IV.4 for datafusion of the photogrammetric equalised digital photo with the corresponding equalised thermogram.

The presented work was funded by the Deutsche Forschungsgemeinschaft (DFG) within the project titled "Structure and moisture investigation of buildings and building elements using impulse-thermography".

References

[1] Kohl C, Maierhofer C, Mayer K, Wöstmann J, Wiggenhauser H. 3D-visualisation of NDT data using a data fusion technique. Insight 2003;45(12):800–8.

[2] Maierhofer C, Krause M, Mielentz F, Streicher D, Milmann B, Gardei A, et al. Complementary application of radar, impact-echo and ultrasonics for testing concrete structures and metallic tendon ducts. Transport Res Rec: J Transport Res Board 2004;1892:170–7. TRB, National Research Council, Washington, DC.

[3] Maierhofer C, Brink A, Röllig M, Wiggenhauser H. Transient thermography for structural investigation of concrete and composites in the surface near region. Infrared Phys Technol 2002;43:271–8.

[4] Maierhofer C, Wiggenhauser H, Brink A, Röllig M. Quantitative numerical analysis of transient IR experiments on buildings. Infrared Phys Technol 2004;46:173–80.

[5] Chown G, Burn K. Thermographic identification of building enclosure defects and deficiencies. Canadian Building Digest 1983.

[6] Maldague XPV. Non-destructive evaluation of materials by infrared thermography. London: Springer-Verlag; 1993.

[7] Danesi S, Salerno A, Wu D, Busse G. Cooling down thermography: principle and results in NDE. In: Snell JR, Wurzbach RN, editors. Proceeding of the international society for optical engineering, Thermosense XX, Orlando, 1998. p. 266–74.

[8] Vavilov V, Kauppinen T, Grinzato E. Thermal characterisation of defects in building envelopes using long square pulse and slow thermal wave techniques. Res Non-Destruct Eval 1997;9:181–200.
[9] Weise F, Arndt D, Borchardt K, Geyer E, Henschen J, Krause M, et al. Non-destructive testing methods for determining the built-in position of anchoring elements at curtain facades. In: Schickert G, Wiggenhauser H, editors. Proceedings of the int. symp. on non-destructive testing in civil engineering (NDT-CE), vol. 1. Berlin: DGZfP; 1995. p. 867–76.
[10] Bjegovic D, Mikulic D, Sekulic D. Non-destructive methods for monitoring of reinforcing steel in concrete. In: Forde MC, editor. Proceedings of 9th int. conf. on structural faults and repair. London: Engineering Technics Press; 2001. CDROM.
[11] Stimolo M. Praktische Anwendung der Thermografie im Straßenbau und für Abdichtungssysteme. DGZfP-Berichtsband 77-CDROM. Thermografie-Kolloquium. Stuttgart: DGZfP; 2001 [in German].
[12] ASTM Standard D4788-88 (reapproved 1997): Standard test method for detecting delaminations in bridge decks using infrared thermography.
[13] Carlomagno GM, Di Maio R, Meola C, Roberti N. Infrared thermography and geophysical techniques in cultural heritage conservation. Quant Infrared Thermogr J 2005;2(1):5–24.
[14] Arndt R, Hillemeier B, Maierhofer C, Rieck C, Röllig M, Scheel H, et al. Zerstörungsfreie Ortung von Fehlstellen und Inhomogenitäten in Bauteilen mit der Impuls-Thermografie. Bautechnik 2004;81(10):786–93 [in German].
[15] Ibarra-Castanedo C, Maldague XPV. Pulsed phase thermography review. Quant Infrared Thermogr J 2005;1(1):47–70.
[16] Weritz F, Arndt R, Röllig M, Maierhofer C, Wiggenhauser H. Investigation of concrete structures with pulse phase thermography. Mater Struct 2005;38:843–9.